The International Journal of Advanced Manufacturing Technology (2019) 101:1197–1213
https://doi.org/10.1007/s00170-018-3002-x

ORIGINAL ARTICLE

Zoom synchrosqueezing transform-based chatter identification in the milling process

Songtao Xi[1] · Hongrui Cao[2] · Xingwu Zhang[1] · Xuefeng Chen[2]

Received: 15 May 2018 / Accepted: 6 November 2018 / Published online: 16 November 2018

Abstract
Self-excited chatter vibration is one of the most unexpected phenomena during the milling operation, which is always combined with time-varying and non-stationary characteristics. This paper presents a milling chatter detection approach combined with the time-frequency analysis (TFA) method and instantaneous frequency and energy aggregation characteristics of the chatter vibration in the milling process. A zoom synchrosqueezing transform (ZST)-based chatter identification approach and several chatter identification indicators are constructed for milling chatter identification. The TFA method ZST is used to characterize the time-varying and non-stationary characteristics of the chatter vibration. The zoom strategy is used to improve the time-frequency resolution and energy concentration of the obtained time-frequency distribution. From an energy aggregation characteristic perspective, 13 instantaneous frequency domain statistic indicators and an instantaneous energy ratio indicator based on the time-frequency distribution obtained by ZST are developed for milling chatter identification. Four groups of cutting tests with both end milling and peripheral milling are conducted to validate the effectiveness of the developed chatter identification indicators, and results show that the developed chatter identification indicators can effectively identify chatter in the milling process and are insensitive to the cutting parameters.

Keywords Milling chatter identification · Zoom synchrosqueezing transform · Time-frequency analysis · Indicators

1 Introduction

Chatter is one of the most unexpected phenomena during the milling operation, which is a severe self-excited vibration that always combined with time-varying and non-stationary characteristics. Chatter occurrence in the machining processes has several negative effects, such as poor surface quality, unacceptable inaccuracy, shortened life of the cutter and machine tool, and excessive noise [1, 2]. Since the regeneration theory of the chatter was proposed in the 1960s, a great deal of studies have been conducted to investigate the chatter in the machining process not only on an analytically study of chatter stability [3–9], but also on chatter detection [10–13] and online active control [14, 15].

Due to the tight coupling and high time-varying properties of the whole cutting system, the analytic methods could not accurately model the cutting system and perfectly prevent the occurrence of chatter in machining. In comparison, the online chatter detection of the milling process based on the vibration signal has more potential value for practical use, as it does not need to consider the coupling and parameter identification of the cutting for system modeling and time-varying properties of the cutting system. Once the chatter is identified, some control strategies, e.g., changing the cutting parameters of the machining process, can be automatically adjusted to make the cutting process in a stable condition.

In order to conduct the cutting status monitor and chatter identification, various kinds of sensors and signals have been utilized, including cutting force [12, 16–20], vibration acceleration and displacement signals [21–25], acoustic emission [16, 17, 26], servo current [27, 28], sound signal [29, 30], etc. Kuljanic et al. [16] presented an investigation on multisensor approaches for chatter identification in the face milling process. Sensors

✉ Hongrui Cao
chr@mail.xjtu.edu.cn

[1] School of Mechanical Engineering, Xi'an Jiaotong University, 710049 Xi'an, People's Republic of China

[2] State Key Laboratory for Manufacturing Systems Engineering, Xi'an Jiaotong University, 710049 Xi'an, People's Republic of China

including rotating dynamometer, accelerometers, acoustic emission, and electrical power sensors were all applied and compared to determine which kinds of signal are sensitive to chatter onset. Chatter detection methods based on force, displacement signals, and machined surface topography in high-speed micromilling were compared by Singh et al. [31].

As important as sensor technologies, in order to realize accurate cutting status monitoring and chatter onset detection as early as possible, efficient signal processing algorithm is another critical issue that should be carefully considered. A lot of researchers have conducted significant studies on the signal processing algorithm for chatter detection, and methods in time domain [27, 30, 32], frequency domain [18, 24, 33], and time-frequency domain [20, 21, 25, 29, 34] have all been presented and investigated. In time domain methods, Li et al. [35] proposed a time domain method using the coherence function of two crossed acceleration signals to identify chatter and tool wear in turning processes. Results showed that the normalized coherence function was close to unity at the onset on chatter and severe tool wear. Yamato et al. [28] proposed to use the power factor theory based on phase monitoring for the turning chatter detection in the time domain without additional sensors. Schmitz [30] proposed to use a statistical evaluation of the once per-revolution milling audio signal for milling chatter detection based on a Poincare mapping technique. In frequency domain methods, Lamraoui and Thomas et al. [18, 33] used the cyclostationarity approach for monitoring chatter and tool wear in high-speed milling based on acceleration signals, cutting forces, and instantaneous angular speeds (IAS). Milling chatter is a non-stationary phenomenon, and signals corresponding to milling chatter are full of time-varying properties. Since the traditional time domain method conceals the frequency domain information and the Fourier transform method conceals the time domain information, hence, they are blind to state transition in non-stationary signals and ineffective for online detection of chatter onset. In comparison, the time-frequency domain and non-stationary signal automatic decomposition methods could provide alternative approaches to identify fault features for the non-stationary process. These methods could be classified into two groups. In the first group, the methods are mainly used as a signal preprocessing technology to automatically decompose the non-stationary signals and extract the useful components. These methods include the discrete wavelet transform (DWT) [10, 36], wavelet packet decomposition (WPD) [12, 21, 47], ensemble empirical mode decomposition (EEMD) [22, 24], variation model decomposition (VMD) [12, 48], etc. Then, the extracted useful components will be further processed to construct the chatter detection indicators. In the second group, the time-frequency analysis (TFA) methods are used to obtain the time-frequency distribution of the signal which will be used to construct the chatter detection indicators. Methods such as the Hilbert-Huang transform [21, 24, 32], continuous wavelet transform, short-time Fourier transform [34], and synchrosqueezing transform [29] are included in this group. Sometimes two groups of methods are combined together and used for chatter detection. Cao et al. [21] presented a chatter identification method in the end milling process using wavelet packets and the Hilbert transform. The wavelet packets transform was used as a preprocess approach to denoise the measured signal, and the Hilbert transform is used to obtain the time-frequency energy distribution of the reconstruct signal. The mean value and the standard deviation of the Hilbert-Huang spectrum were used to detect the chatter. Fu et al. [24] proposed an energy aggregation characteristic-based Hilbert-Huang transform method for online chatter detection. The EEMD is used to decompose the measured signal to obtain feature intrinsic mode functions (IMFs) using majority energy rule. The Gaussian mixed model is used to automatically calculate the thresholds.

As milling chatter is a nonlinear and non-stationary phenomenon, some researchers proposed to use entropy and complexity index to reflect the irregularity and complexity of the signal with chatter onset. Daniel et al. [25, 37] proposed to use the approximate entropy (ApEn) to deal with the nonlinear and non-stationary data in milling operation and to identify chatter instability. Gradišek et al. [19] used the coarse-grained entropy rate of the cutting forces' signals to detect chatter in the turning process and found that a high value of the entropy rate is typical for chatter-free cutting, while for chatter a low value is typical.

Sometimes, the entropy and complexity index are combined with the abovementioned TFA methods for milling chatter identification. Cao et al. [22] presented a chatter identification method in the end milling process based on EEMD and nonlinear dimensionless indicators. First, the EEMD is used to decompose the comb-filtered signal to obtain the sensitive IMFs contacting rich chatter information. Then, two nonlinear dimensionless indicators, i.e., C_0 complexity and power spectral entropy, of the selected sensitive IMFs were calculated to identify the chatter in milling operations. Rafal et al. [32] proposed to use the time forces and torque series measured by a rotating dynamometer during the milling process for chatter identification. The recurrence plot (RP) technique, HHT, and approximate entropy were used to analyze the measured force and torque signals and detect the chatter in the milling process. Zhang et al. [12] proposed to use the energy entropy combined with the VMD and WPD for the chatter detection in milling operation.

Some authors considered the chatter from the energy aggregation characteristic perspective, and pointed out that chatter is a phenomenon reflecting changes of frequency and energy distribution in the machining process. Based on this perspective, many significant researches have been conducted. Uekita et al. [34] proposed to use the short-time Fourier transform (STFT) combined with spectral kurtosis (SK) analysis in the time-frequency domain to identify chatter and transient vibration information from an acceleration signal during the deep-hole drilling process.

As for chatter identification based on the energy aggregation perspective, how to accurately reflect the change of the spectrum and energy distribution of the signal with chatter onset is of great importance. Appropriate signal processing method which can provide good time-frequency resolution and energy concentration time-frequency distribution, and appropriate indicators which can effectively reflect the change of the spectrum and energy distribution of the signal with chatter onset is of great importance.

This study focuses on the milling chatter identification based on the energy aggregation perspective. A novel effective TFA method named zoom synchrosqueezing transform (ZST) is adopted to obtain the time-frequency distribution (TFD) of the measured vibration signal. ZST is an improvement of the synchrosqueezing transform (ST). ST proposed by Daubechies et al. [38] is a powerful TFA method that can efficiently improve the readability of the TFD with time-varying frequency. Based on the original ST, several improvement algorithms have been proposed and used for instantaneous speed estimation and mechanical fault diagnosis of rotating machinery, such as generalized syschrosqueezing transform (GST) [39], second-order synchrosqueezing transform [40], frequency-shift synchrosqueezing [41], ZST [42, 43], and the matching demodulation transform and synchrosqueezing [44]. ZST is a powerful TFA method which can provide both excellent time and frequency resolution, and good energy concentration TFD.

In this study, ZST is used to accurately display the instantaneous spectrum and energy distribution, and to obtain accurate TFD of the signal with both excellent time and frequency resolution and good energy concentration. Then, from the frequency and energy aggregation perspective of the chatter vibration, 13 instantaneous frequency domain indicators and an instantaneous energy ratio indicator based on the TFD obtained by ZST are presented and compared to find which indicators are more effective to reflect the change characteristics of the instantaneous spectrum and energy distribution of the signal with chatter onset. Four groups of cutting tests with both end milling and peripheral milling are conducted to validate the effectiveness of the developed chatter identification indicators.

2 Zoom synchrosqueezing transform-based chatter identification

2.1 Algorithm of short-time Fourier transform-based ZST

As the CWT-based ZST has been introduced in detail in [42], the STFT-based ZST is presented here.

2.1.1 STFT-based ST

The modified STFT is used in the STFT-based synchrosqueezing transform. For a given signal $x(t)$, the modified short-time Fourier transform is defined by:

$$S_x^g(u,\xi) = \int_{-\infty}^{\infty} x(t) g(t-u) e^{-i2\pi\xi(t-u)} dt \tag{1}$$

where $g(t)$ is the window function. Different from the traditional STFT, the modified short-time Fourier transform is modulated by a modulation factor $e^{i2\pi\xi u}$.

Consider signal $x(t) = A\cos(\omega_0 t)$ as a purely harmonic signal. By Plancherel's theorem, the STFT of signal $x(t)$ can be rewritten in the frequency domain as:

$$\begin{aligned} S_x^g(u,\xi) &= \int_{-\infty}^{\infty} x(t) g(t-u) e^{-i2\pi\xi(t-u)} dt \\ &= \frac{1}{2\pi}\int_{-\infty}^{\infty} F(\omega)\overline{G(\varpi-\omega)e^{-i\varpi u}} d\varpi \\ &= \frac{1}{2\pi}\int_{-\infty}^{\infty} \delta(\varpi-\omega_0) G(\varpi-\omega) e^{i\varpi u} d\varpi \\ &= \frac{A}{2\pi} e^{i\omega_0 u} G(\omega_0-\omega) \end{aligned} \tag{2}$$

where $F(\omega)$ is the Fourier transform of $x(t)$ and $\overline{G(\varpi-\omega)e^{-i\varpi t}}$ is the complex conjugate of the Fourier transform of the modulated window function $g(t-u)e^{-i2\pi\xi u}$. Then, from Eq. (2), the following equation can be obtained by calculating the partial derivative of $S_x^g(u,\xi)$ to u:

$$\frac{\partial}{\partial u} S_x^g(u,\xi) = i\omega_0 \frac{A}{2\pi} e^{i\omega_0 u} G(\omega_0-\omega) = i\omega_0 S_x^g(u,\xi) \tag{3}$$

For any (u,ξ) satisfying $S_x^g(u,\xi) \neq 0$, a candidate IF of signal $x(t)$ can be obtained by:

$$\widehat{\omega_x}(u,\xi) = \omega_0 = \frac{\partial_t S_x^g(u,\xi)}{i S_x^g(u,\xi)} = -i\left(S_x^g(u,\xi)\right)^{-1} \frac{\partial}{\partial t} S_x^g(u,\xi) \tag{4}$$

Finally, the discrete form of the STFT-based synchrosqueezing transform can be obtained based on the calculated candidate IF:

$$T_s(u,\omega_l) = \sum_{k:|\widehat{\omega_x}(u,\xi_k)-\omega_l| \le \Delta\omega/2} S_x^g(u,\xi_k)(\Delta\xi) \tag{5}$$

where ξ_k is the discrete frequency series, with $\Delta\xi = \xi_k - \xi_{k-1}$. The synchrosqueezing transform is likewise determined only

at the center frequency ω_l of the successive bins: $[\omega_l - 1/2\Delta\omega, \omega_l + 1/2\Delta\omega]$, with $\Delta\omega = \omega_l - \omega_{l-1}$ and $S_x^g(u,\xi_k) \geq \gamma \geq 0$.

2.1.2 STFT-based zoom synchrosqueezing transform

In most cases, for a considered signal, only a certain frequency band of the signal is valuable or useful to us. Thus, we only need to analyze the useful components of the signal in the specific frequency band and do not need to pay much attention to the whole frequency band. The idea of the ZST is to obtain both excellent time and frequency resolution to analyze the signal in a selected frequency range, so as to accurately display the time-varying characteristics of the signal and obtain good energy concentrated TFD.

For a selected frequency band $[f_m, f_M]$ which includes the concerned frequency components of the signal, the final discrete frequency sequence of the ZST-TFD is defined as:

$$f_{zs}^*(l) = f_m + \frac{l}{na}(f_M - f_m), \quad l = 0, 1, 2\cdots, na. \tag{6}$$

where na is the total number of the frequency bins in the ZST-TFD, which can be determined according to the actual need for frequency resolution.

Then, the discrete angular frequency sequence can be written as:

$$\omega_{zs}^*(l) = 2\pi f_m + \frac{l}{na}(2\pi f_M - 2\pi f_m), \quad l = 0, 1, 2\cdots, na. \tag{7}$$

Finally, the discrete form of the STFT-based ZST can be obtained:

$$T_{zs}\left(u, \omega_l^*\right) = \sum_{k:\left|\widehat{\omega}_x(u,\xi_k) - \omega_{zs}^*(l)\right| \leq \Delta\omega_{zs}^*/2} S_x^g(u,\xi_k)(\Delta\xi) \tag{8}$$

In this way, the frequency sequence of the considered frequency is refined and the instantaneous energy of the signal can be squeezed into a much more accurate instantaneous frequency location, which can largely improve the frequency resolution as well as the energy concentration of the obtained TFD. As for the improvement of the time resolution, the STFT-based ZST is proposed to use the window function with a much smaller width so as to obtain better time resolution for the analysis of the signal. This differs from the CWT-based ZST which improves the time resolution of the TFD by the frequency-shift method [42]. In the proposed method, the Gaussian function:

$$g(t) = \left(\pi\sigma^2\right)^{-1/4} e^{-t^2/\left(2\sigma^2\right)} \tag{9}$$

is used as window function for the STFT-based ST and ZST. The standard deviation σ of the Gaussian function is used to determine the width of the Gaussian function. The smaller the value of σ, the smaller the width of the Gaussian function and as well as better time resolution can be obtained.

2.1.3 Simulation case study

A simulation signal is defined as:

$$\begin{aligned} x(t) = {} & \sin(2\pi 600t + 0.2\sin(2\pi 10t)) \\ & + \sin(2\pi 650t + 0.2\sin(2\pi 10t))(t > 1) \\ & + \sin(2\pi 700t) + \sin(2\pi 750t)(t > 2) \end{aligned} \tag{10}$$

The time domain waveform, STFT-based ST-TFD and the STFT-based ZST-TFD with a zoom frequency band (550–800 Hz) are shown in Fig. 1. In this case, the Gaussian window function defined in Eq. (9) with $\sigma = 0.02$ is used.

From Fig. 1, it can be seen that due to the relative bad time and frequency resolution, the instantaneous frequency function of the frequency demodulation components in the signal cannot be accurate characterized by the STFT-based ST. While as the STFT-based ZST can provide both excellent time and frequency resolution, the IF of the demodulation components can be accurately characterized by the STFT-based ZST with much better energy concentration.

2.2 ZST-based chatter identification indicator construction

2.2.1 Chatter mechanism

Chatter vibration in the milling process is a complex phenomenon which can cause great negative effects. The stability lobe diagram (SLD) theory has been widely investigated for cutting stability prediction, which can provide the border between the stable cut and unstable cut with chatter in the form of axial depth of cut as a function of the spindle rotating speed [3, 4]. According to the SLD theory, the region below the border of the SLD is the chatter-free region, and the region above is the unstable chatter region. In the chatter-free region of the SLD, the energy of the tool is dominated by tooth passing frequency (TPF) and its harmonics, and with the increase of the cutting depth, the cutting force between the tool and workpiece increases. As a result, the amplitude of the TPF and its harmonics increase. When the cutting depth increases and reaches the border of the SLD under certain cutting conditions, chatter occurs. When chatter occurs, abnormal frequency components (i.e., the chatter frequencies) appear on the spectrum of the dynamic vibration signal. With further increase of the cutting depth, chatter vibration aggravates and the amplitude of abnormal chatter frequencies increases sharply and finally dominates the frequency spectrum. During this procedure, the frequency and energy distribution of the spectrum change sharply. This is the intrinsic difference between

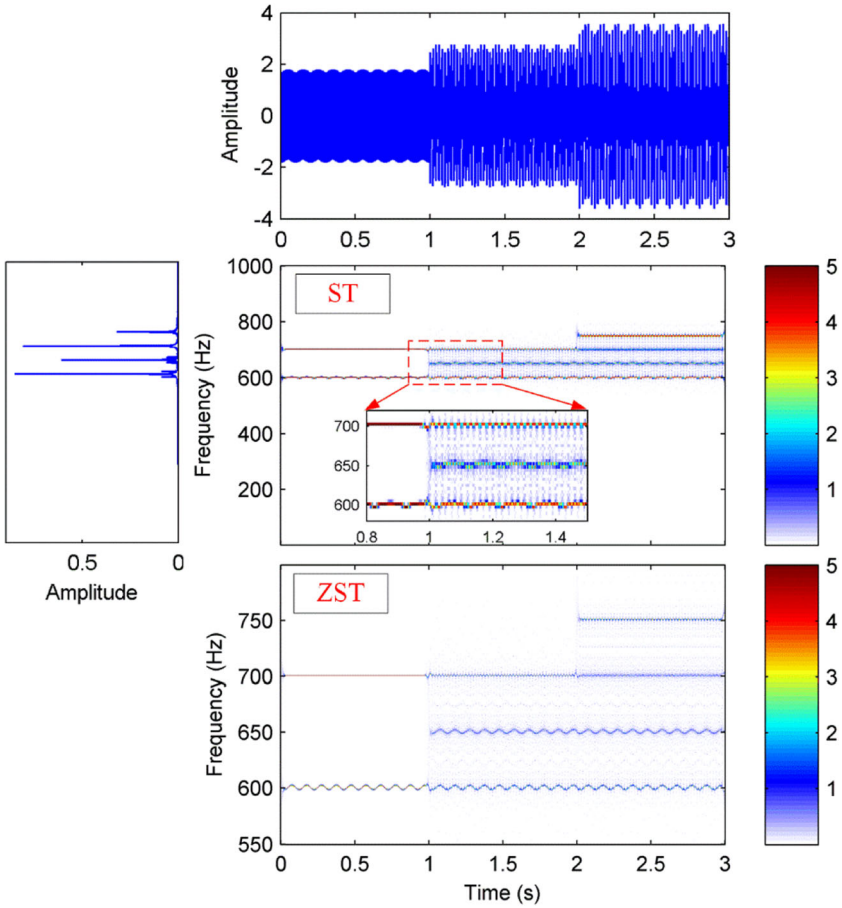

Fig. 1 The time domain waveform, STFT-based ST, and ZST TFDs of the simulation signal

the stable chatter-free and unstable chatter signals, and is the main characteristic for the chatter identification.

What should be noted is that both the amplitude of the chatter frequencies and TPF and its harmonics increase with the onset and aggravation of chatter. The neglect of the amplitude increase of the spindle rotational frequency (SRF) and its harmonics will decrease the insensitivity of the TFA-based chatter identification indicators to the cutting parameters.

Additionally, a special cutting condition is seldom considered in the current TFA-based chatter identification methods. In this cutting condition, one of the harmonics of the TPF is equal to or much close to the natural frequency of the tool-workpiece coupling system. The critical cutting depth reaches the peak (local maximum value) of the SLD at the corresponding spindle speed. In this case, although in stable chatter-free cutting condition, in the higher frequency region of the spectrum near the certain order natural frequency of the system (which is sensitive frequency band for chatter frequencies in ordinary cutting conditions), the amplitude of the TPF harmonics gradually domain the spectrum with the increase of the cutting depth. This special phenomenon has been introduced in detail by Altintas and Weck [5] and Niels et al. [14]. Niels et al. [14] applied this theory to active chatter control in the high speed milling process. However, this special condition is seldom considered in current TFA-based chatter identification methods, e.g., the energy ratio indicator. Thus, the effectiveness of the proposed TFA-based chatter identification indicators will be weakened without the consideration of this special cutting condition.

Based on the time-varying and non-stationary characteristic, a ZST-based chatter identification approach and several chatter identification indicators are constructed for milling chatter identification. The ZST is used to accurately characterize the time-varying and non-stationary characteristics of the chatter vibration. The Zoom strategy is used to improve the time-frequency resolution and energy concentration of the obtained time-frequency distribution.

2.2.2 ZST-based indicators construction for chatter identification

Firstly, chatter vibration in the milling process is highly time-varying and non-stationary, which is suitable to be analyzed by the TFA method to accurately represent the time-varying and non-stationary characteristics of the signal. Secondly, the change of instantaneous frequency and energy distribution is the intrinsic difference between the stable chatter-free and unstable chatter signals, which is the most conspicuous

characteristic for the chatter identification. Based on these two factors, frequency domain statistic indicators based on the ZST TFA method have been constructed and applied to detect the transient changes of the cutting conditions so as to realize the identification of the milling chatter.

As noted by Obuchowski et al. [45], it is of great significance to enhance readability before performing feature extraction and decision-making. In this study, the ZST is presented to enhance the time-frequency resolution and energy concentration property before the feature extraction for chatter identification. Then, ZST-TFD-based frequency domain statistic indicators are calculated and used to reflect the frequency and energy distribution change of each transient of the cutting process.

In order to remove the effect of the cutting parameters on the chatter identification indicators and consider the special cutting case mentioned in section 2.2.1, the harmonics components of the SRF (including the harmonics of the SRF and TPF) are filtered out from the ZST-TFD.

The harmonics of the SRF of the ZST-TFD are filtered with a certain frequency band by the following approach:

$$T_{zsf}(t_i,f_k)=T_{zs}\left(t_i,f_k\right)\Big|_{\{f_k\in[nF_r-\Delta f/2,nF_r+\Delta f/2]\}} =0,\quad n=0,1,2,\cdots \tag{11}$$

where F_r is the SRF and Δf is the width of the filter frequency band.

According to the statement of the chatter mechanism in section 2.2.1, we find that when chatter occurs the frequency components and energy distribution of the spectrum of the vibration signal change. These changes mainly happen in the frequency band which includes the system natural frequencies, and we call this frequency band as the sensitive frequency band.

Thirteen instantaneous frequency domain statistic chatter identification indicators based on the filtered TFD of the ZST, i.e., the TFD without the harmonics of the SRF, are presented and investigated to find which indicators are effective for milling chatter identification. The definition of the 13 frequency domain statistic indicators are given in Table 1.

In Table 1, K denotes the total number of the frequency bins in the selected frequency band, f_k denotes the k^{th} frequency value of the selected frequency band, and $S_{zs}(k)$ denotes the amplitude corresponding to the frequency f_k, i.e., $S_{zs}(k)=T_{zsf}(t_i,f_k)$. All these parameters are calculated at a considered transient t_i, i.e., a column of the ZST-TFD matrix.

In these 13 frequency domain statistical indicators, P_1 is the mean value of the amplitude of the filtered instantaneous spectrum in the sensitive frequency band at a considered transient t_i, which is used to reflect the chatter vibration energy in the sensitive frequency band. When the cutting condition is stable, there is only noise left on the filtered instantaneous spectrum in the sensitive frequency band (as the harmonics of the spindle rotating frequency and tooth passing frequency have been filtered, and there is no chatter frequencies). The mean value of the amplitude of the filtered instantaneous spectrum in the sensitive frequency band is very small. However, when chatter occurs, there are lots of chatter frequencies on the filtered instantaneous spectrum in the sensitive frequency band. Thus, the mean value P_1 of the amplitude of the filtered instantaneous spectrum in the sensitive frequency band increases and becomes a large value.

P_2 is the variance of the amplitude of the filtered instantaneous spectrum in the sensitive frequency band and is used to reflect the concentrative degree of the amplitude of the filtered instantaneous spectrum in the sensitive frequency band. P_3 is the definition of kurtosis, which is used as a descriptor of the shape of the amplitude of the filtered instantaneous spectrum in the sensitive frequency band. P_4 is the definition of skewness, and it is used as a measure of the asymmetry of the amplitude of the filtered instantaneous spectrum in the sensitive frequency band. Additionally, other statistical indicators were firstly defined to reflect the frequency and energy distribution of the spectrum for fault identification of the rotating machinery. In this paper, these statistical indicators are adopted for chatter identification. Indicators P_6 and $P_{10}-P_{13}$ are used to reflect the concentration or dispersion degree of the filter instantaneous spectrum in the sensitive frequency band. Indicators P_5 and P_7-P_9 are used as descriptors of the position change of the main frequency band with the major in the filter instantaneous spectrum in the sensitive frequency band.

The schematic diagram of the ZST-based instantaneous frequency domain statistic indicators construction for milling chatter identification is given in Fig. 2. According to the regeneration chatter theory, chatter frequencies mainly appear around the system natural frequencies. In this study, the sensitive frequency band where chatter frequencies always appear, i.e., the frequency band includes main natural frequencies of the system, is selected as the zoom frequency band.

The zoom frequency band can be selected based on the tool-tip frequency response function (FRF) test or the analysis of the measured chatter vibration signal. The principle of the frequency band selection for ZST is that the main mode natural frequencies which mainly lead to chatter vibration should be included. Additionally, the frequency band should include least harmonics of TPF that has prominent amplitude in stable cutting conditions, which can improve the time-frequency resolution and energy concentration of the obtained ZST-TFD. The ZST is used to enhance the time-frequency resolution and energy concentration property before the feature extraction for chatter detection. Based on the obtained ZST-TFD, frequency domain statistic indicators are calculated and used to reflect the instantaneous frequency and energy distribution change of

Table 1 Definition of the 13 frequency domain statistic indicators

Indicators		
$P_1 = \frac{\sum_{k=1}^{K} S_{zs}(k)}{K}$	$P_2 = \frac{\sum_{k=1}^{K} (S_{zs}(k)-P_1)^2}{K-1}$	$P_3 = \frac{\sum_{k=1}^{K} (S_{zs}(k)-P_1)^4}{K}$
$P_4 = \frac{\sum_{k=1}^{K} (S_{zs}(k)-P_1)^3}{K}$	$P_5 = \frac{\sum_{k=1}^{K} f_k S_{zs}(k)}{\sum_{k=1}^{K} S_{zs}(k)}$	$P_6 = \sqrt{\frac{\sum_{k=1}^{K} (f_k-P_5)^2 S_{zs}(k)}{K}}$
$P_7 = \sqrt{\frac{\sum_{k=1}^{K} f_k^2 S_{zs}(k)}{\sum_{k=1}^{K} S_{zs}(k)}}$	$P_8 = \sqrt{\frac{\sum_{k=1}^{K} f_k^4 S_{zs}(k)}{\sum_{k=1}^{K} f_k^2 S_{zs}(k)}}$	$P_9 = \frac{\sum_{k=1}^{K} f_k^2 S_{zs}(k)}{\sqrt{\sum_{k=1}^{K} S_{zs}(k) \sum_{k=1}^{K} f_k^4 S_{zs}(k)}}$
$P_{10} = \frac{P_6}{P_5}$	$P_{11} = \frac{\sum_{k=1}^{K} (f_k-P_5)^3 S_{zs}(k)}{K P_6^3}$	$P_{12} = \frac{\sum_{k=1}^{K} (f_k-P_5)^4 S_{zs}(k)}{K P_6^4}$
$P_{13} = \frac{\sum_{k=1}^{K} (f_k-P_5)^{1/2} S_{zs}(k)}{K\sqrt{P_6}}$		

each transient of the cutting process. Then, the change of the frequency and energy distribution over time can be obtained.

2.2.3 Energy ratio chatter identification indicator based on ZST

With the onset and aggravation of the chatter, not only the frequency distribution but also the energy distribution or energy ratio between the chatter frequencies and the normal TPF and its harmonics of the signal instantaneous spectrum change. Thus, some researchers have conducted a significant investigation on the energy ratio indicator for chatter identification both in milling [24] and turning [46] operations. However, the special cutting condition mentioned in section 2.2.1 is seldom considered in the current presented energy ratio indicators for chatter identification. The neglect of the special cutting case will weaken the effectiveness of the current energy ratio indicators.

In this study, an improved energy ratio indicator based on ZST is developed for chatter identification in high-speed milling operation. In the proposed energy ratio indicator, the special stable cutting condition is considered by filtering out the effect of the harmonics of SRF. The energy ratio indicator is defined as the ratio of instantaneous total energy of the chatter frequencies in ZST-TFD to the instantaneous total energy of the signal.

For a considered transient t_i, the total energy of the harmonics of SRF E_{zstp} in the ZST-TFD can be calculated by the following equation:

$$E_{zstp} = \sum_{\{f_k \in [nF_r - \Delta f/2, nF_r + \Delta f/2] \cap [f_m, f_M]\}} S_{zs}(k), \quad n = 0, 1, 2, \cdots; k = 1, 2, \cdots na; \tag{12}$$

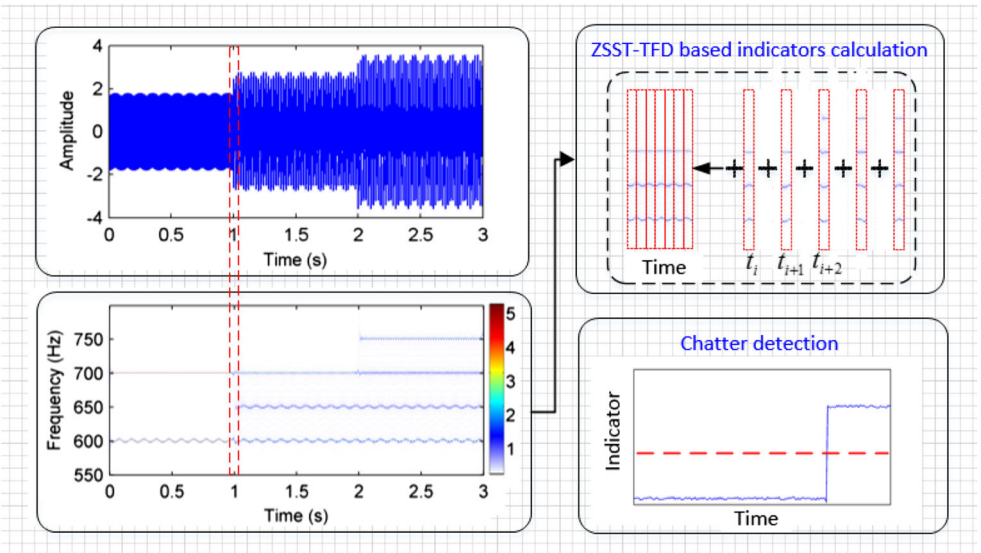

Fig. 2 The schematic diagram of the ZST-based instantaneous frequency domain statistic indicators construction for milling chatter identification

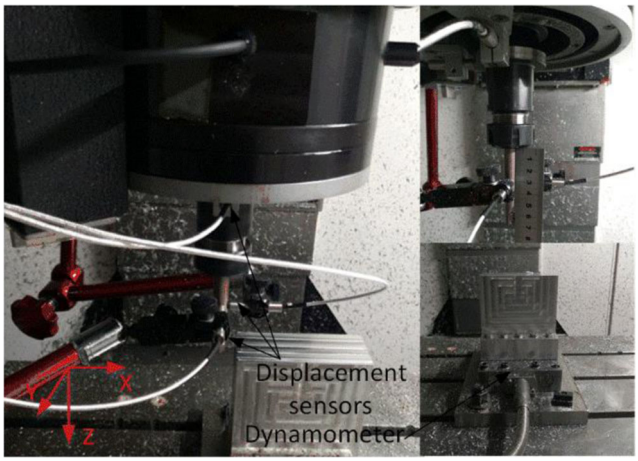

Fig. 3 The experiment setup for end milling

The total instantaneous energy of the ZST-TFD and ST-TFD at transient t_i is calculated respectively by:

$$E_{zsto} = \sum_{\{f_k \in [f_m, f_M]\}} S_{zs}(k), \quad k = 1, 2, \cdots \tag{13}$$

$$E_{sto} = \sum_{\{f_l \in [0, f_s/2]\}} S_s(l), \quad l = 1, 2, \cdots. \tag{14}$$

Then, the total energy corresponding to the chatter frequencies and noise in ZST-TFD can be obtained by:

$$E_{zsc} = E_{zsto} - E_{zstp} \tag{15}$$

Finally, the energy ratio indicator defined as the ratio of instantaneous total energy of the chatter frequencies in ZST-TFD to the instantaneous total energy of the signal is defined as:

$$ER_{zs} = E_{zsc}/E_{sto} \tag{16}$$

3 Validation and application

3.1 Experiment setup introduction

In order to validate the effectiveness of the developed chatter identification indicators, cutting tests were carried out on a CNC milling machine. Both end milling and peripheral milling tests were conducted with two different kinds of milling cutter. A single-blade milling cutter was used for end milling condition and a three-fluted milling cutter was used for peripheral milling condition. The tests were conducted by milling an aeronautical aluminum alloy 7075 workpiece, and all tests were conducted without coolant. Both cutters have a diameter of 12 mm and installation overhang of 70 mm. The cutting forces during the milling operation were collected by a Kistler dynamometer 9129AA, and the vibration displacement signals of the tool and tool holder were measured using the Lion non-contact capacitive displacement sensors (CPL290 with sensitivity as 80 mV/μm). The signals were recorded by an ECON data acquisition system. The sampling frequency was 6000 Hz. The displacement signals were used to identify the chatter onset. The experiment setup for the end milling is shown in Fig. 3. Three groups of end milling cutting tests were conducted, and the corresponding cutting parameters are listed in Table 2. One group of peripheral milling was conducted, and the corresponding parameters are given in Table 3.

Table 2 Cutting conditions for end milling

Group	Test	Milling type	Axial depth of cut (mm)	Radial depth of cut (mm)	Feed rate (mm/min)	Spindle speed (r/min)	Milling method (end or peripheral milling)	Cutting condition
I	a1	Up	0.2	5	300	6500	End milling	Stable
	a2	Up	0.4	5	300	6500	End milling	Stable
	a3	Up	0.6	5	300	6500	End milling	Chatter
	a4	Up	0.8	5	300	6500	End milling	Chatter
	a5	Up	0.9	5	300	6500	End milling	Chatter
	a6	Up	1.2	5	300	6500	End milling	Chatter
II	b1	Up	0.2	10	300	6500	End milling	Stable
	b2	Up	0.4	10	300	6500	End milling	Stable
	b3	Up	0.6	10	300	6500	End milling	Chatter
	b4	Up	0.8	10	300	6500	End milling	Chatter
	b5	Up	0.9	10	300	6500	End milling	Chatter
III	c1	Up	0.2	5	300	4000	End milling	Stable
	c2	Up	0.4	5	300	4000	End milling	Stable
	c3	Up	0.6	5	300	4000	End milling	Stable
	c4	Up	0.8	5	300	4000	End milling	Stable

Table 3 Cutting conditions for peripheral milling

Group	Test	Milling type	Axial depth of cut (mm)	Radial depth of cut (mm)	Feed rate (mm/min)	Spindle speed (r/min)	Milling method (end or peripheral milling)	Cutting condition
IV	d1	Up	10	0.2	1500	6200	Peripheral milling	Stable
	d2	Up	10	0.5	1500	6200	Peripheral milling	Stable
	d3	Up	10	1	1500	6200	Peripheral milling	Stable
	d4	Up	10	2	1500	6200	Peripheral milling	Chatter
	d5	Up	10	2.5	1500	6200	Peripheral milling	Chatter
	d6	Up	10	3	1500	6200	Peripheral milling	Chatter

3.2 Results and discussion

In the first three cutting groups, as the cutter has only one blade, the TPF is equal to the SRF. The time domain waveform and spectrum of the displacement signals under different cutting conditions in the cutting group I are shown in Fig. 4.

From Fig. 4, it can be seen that the amplitude of the time domain waveform of the displacement signal increases with the increase of the axial cutting depth. When the cutting processes are stable, the spectrums of the displacement signals are mainly composed of the harmonics of the TPF in the low-frequency region, and there is only a few TPF component in

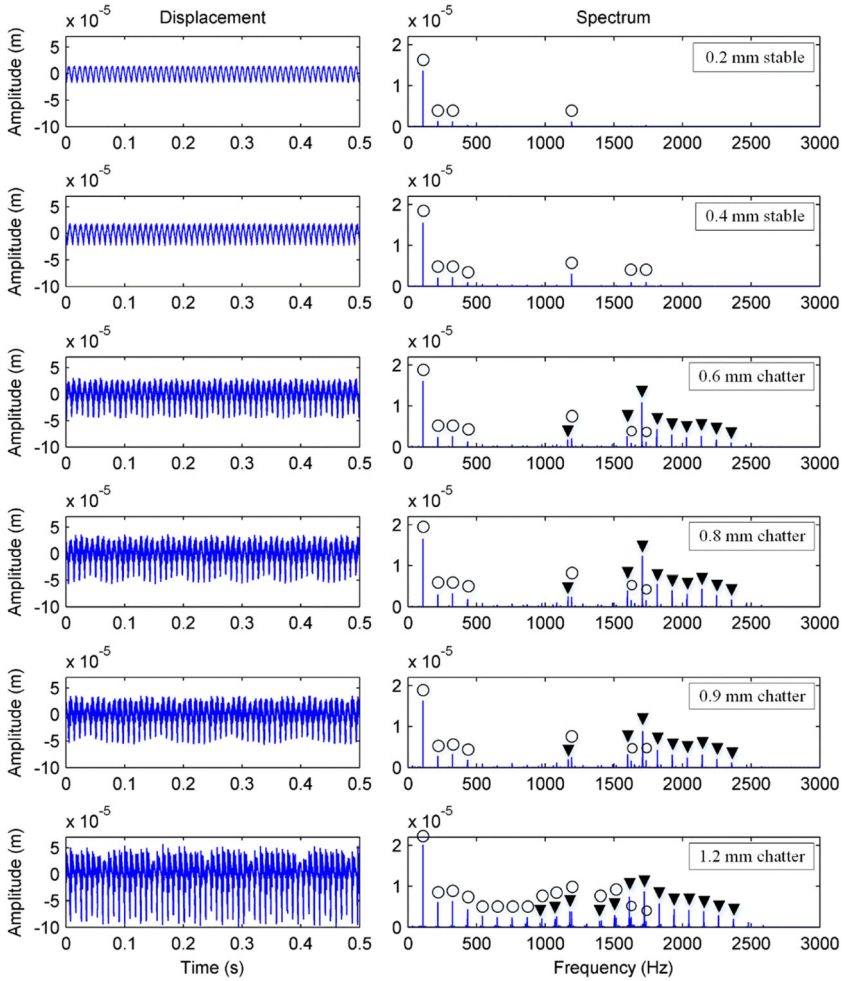

Fig. 4 The time domain waveform and spectrum of the displacement signals under different cutting conditions in the cutting group I (*white circle* the harmonics of the tooth passing frequency, *black down-pointing triangle* the chatter frequencies)

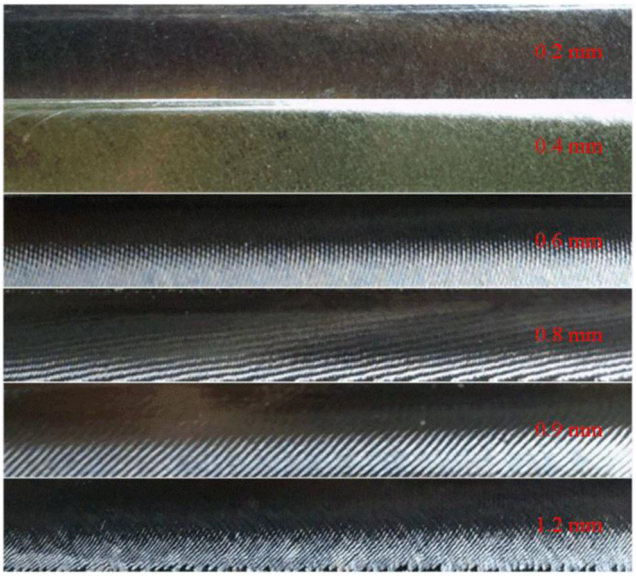

Fig. 5 The finished workpiece surfaces under different cutting conditions in the cutting group I

the high-frequency region. The amplitudes of the harmonics of TPF increase with increase of the axial cutting depth.

With the onset of the chatter, a lot of abnormal chatter frequency components appear in the high-frequency region of the signal spectrum. With the aggravation of the chatter, the amplitudes of the chatter components as well as the number of the chatter frequencies increase with the increase of the axial cutting depth. Additionally, the amplitudes of the TPFs also increase with the increase of the axial cutting depth, as shown in Fig. 4.

The finished workpiece surfaces of six different cutting conditions are shown in Fig. 5. From Fig. 5, it can be seen that when axial cutting depths are 0.2 and 0.4 mm, the cutting process is much stable, and the finished workpiece surface is very good. When the axial cutting depth increased to 0.6 mm, chatter vibration occurs and the cutting process becomes unstable, and there are slight chatter marks left on the finished workpiece surface. With the increase of the axial cutting depth as well as the aggravation of the chatter, the chatter marks become more and more serious and the finished surfaces become worse and worse, as shown in Fig. 5.

The filtered ZST-TFD of the displacement signals under different cutting conditions in the cutting group I is shown in Fig. 6. From Fig. 6, it can be seen that when the cutting condition is stable the filtered ZST-TFD is composed of noise with little amplitude, while when chatter vibration occurs abnormal chatter frequencies appear in the ZST-TFD. With aggravation of the chatter vibration, both the number and amplitude of the chatter frequencies in the ZST-TFD increase.

The 13 instantaneous frequency statistic indicators for chatter identification are calculated based on the ZST-TFD shown in Fig. 6, and the results are given in Fig. 7. From Fig. 7, it can be seen that the indicators P1, P2, P6, P10, P12, and P13 can provide clear identification between stable milling and unstable milling with chatter vibration.

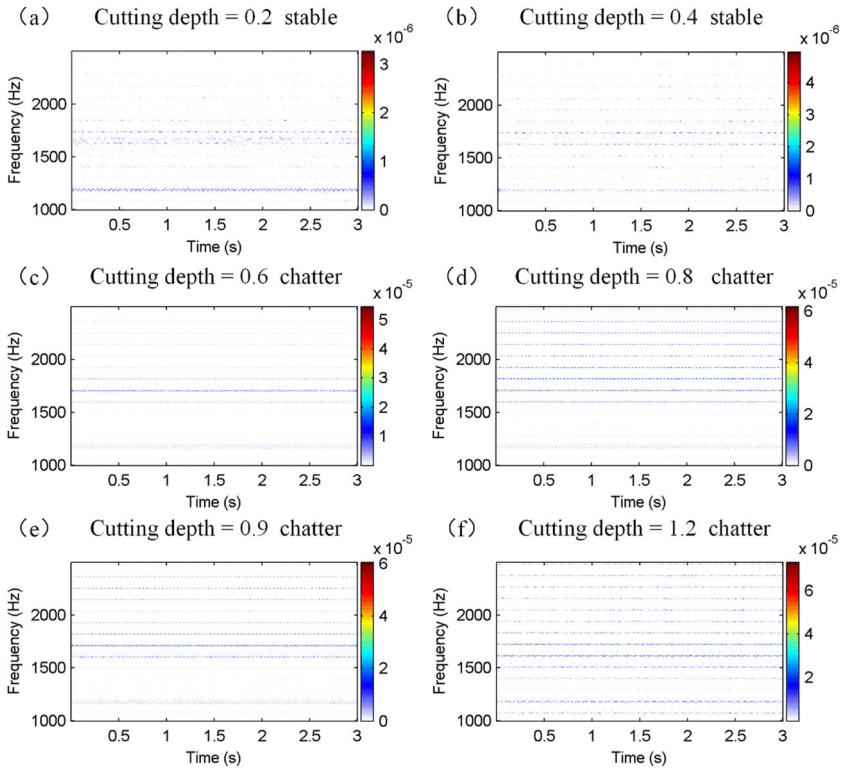

Fig. 6 Filtered ZST-TFD of displacement signals under different cutting conditions in group I

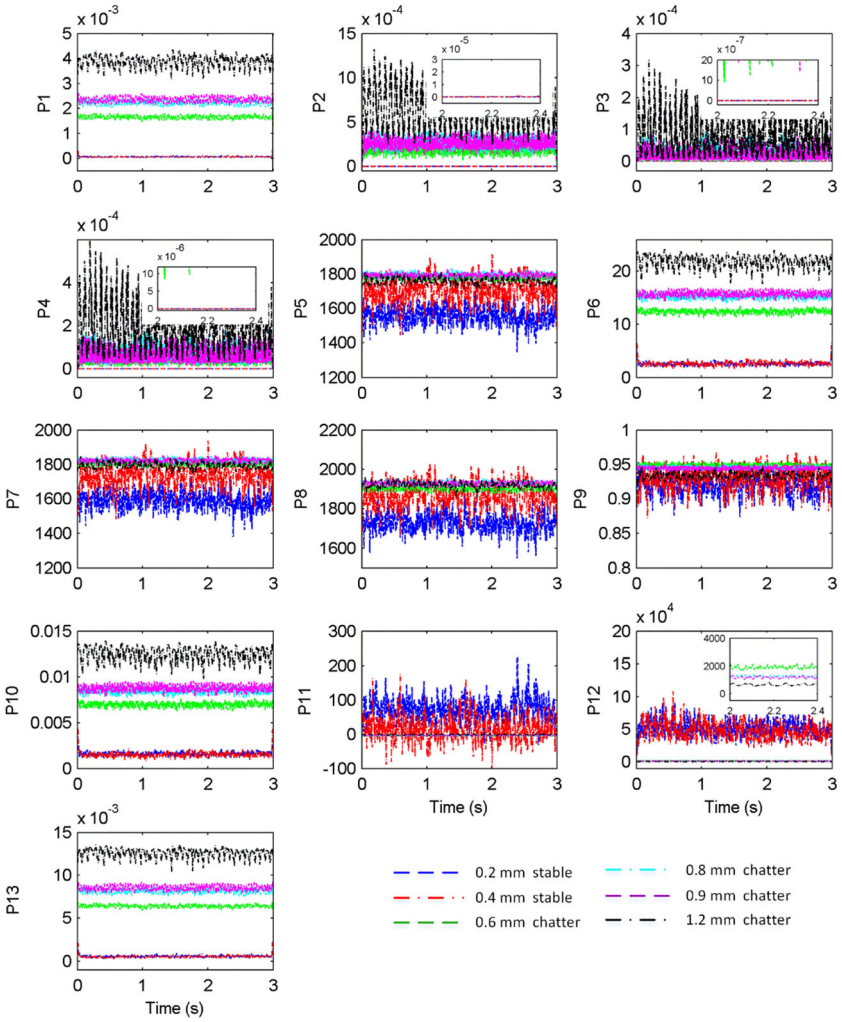

Fig. 7 The 13 frequency domain statistic indicators calculation results of different cutting conditions in the cutting group I

As the TPF components have been filtered out, the influence of the cutting parameters on the indicator calculation results in the stable cutting condition can be effectively removed. When the cutting condition is stable, the indicators calculation results of P1, P2, P6, P10, and P13 in stable cutting conditions are much smaller compared with the indicator calculated results in unstable condition with chatter vibration, as shown in Fig. 7. Take indicator P1 as an example; P1 denotes the mean value of the amplitude of the instantaneous spectrum on the filtered ZST-TFD. When the cutting condition is stable, the filtered ZST-TFD is mainly composed by noise, and the mean value of the amplitude of the instantaneous spectrum is very small and approaches zero. With the onset and aggravation of the chatter, chatter frequencies appear in the higher frequency region and their amplitude increases sharply. As a result, the mean value of the instantaneous spectrum amplitude increases sharply with the aggravation of the chatter vibration, as shown in Fig. 7. The P2 indicator is the variance of the instantaneous spectrum of the filtered ZST-TFD. In stable milling conditions, the filtered ZST-TFD mainly consists of noise which is distributed in the whole zoom frequency region; thus, the variance of the instantaneous spectrum is very small and less than 1.5×10^{-6}. With the onset and aggravation of chatter and appearance of the chatter frequencies, the variance of the instantaneous spectrum increases and is much bigger than that in stable milling conditions, as shown in Fig. 7.

As for the indicator P12, it is much different from the indicator explained above, and it has a much larger value in stable cutting conditions and much smaller value in unstable chatter conditions. When the milling conditions are stable, the values of P12 are always larger than 6×10^3 and fluctuate with very large amplitude, while in unstable chatter milling conditions, the values of P12 are always smaller than 2.5×10^3, and the fluctuation amplitude is very small.

Additionally, the kurtosis P3 and skewness P4 of the instantaneous spectrum of the signal at a considered transient can also effectively identify the stable and unstable chatter

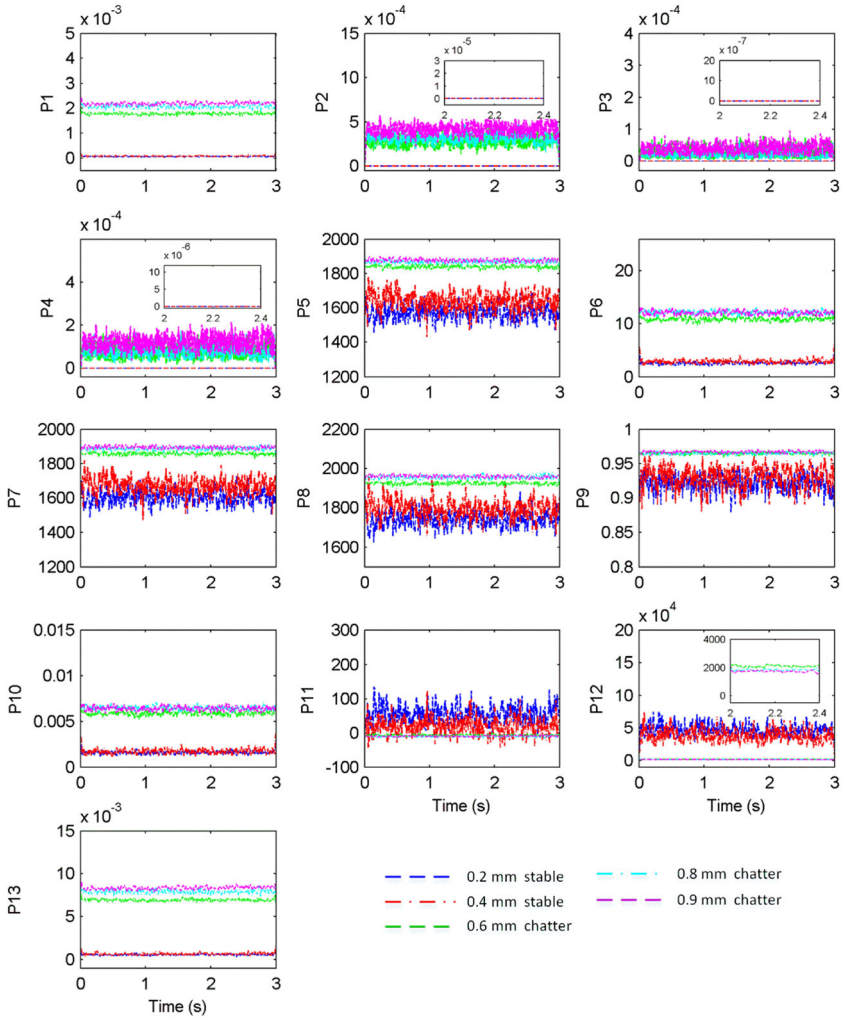

Fig. 8 The 13 frequency domain statistic indicators calculation results of different cutting conditions in the cutting group II

milling conditions. As shown in the partial enlarged detail in Fig. 7, the kurtosis P3 and skewness P4 are almost equal to zero when the cutting condition is stable. Although the value of the kurtosis P3 and skewness P4 is also very small when the milling condition is unstable and chatter, those values are much larger than that of stable cutting conditions. Thus, the kurtosis P3 and skewness P4 can also be used for chatter identification in milling operation.

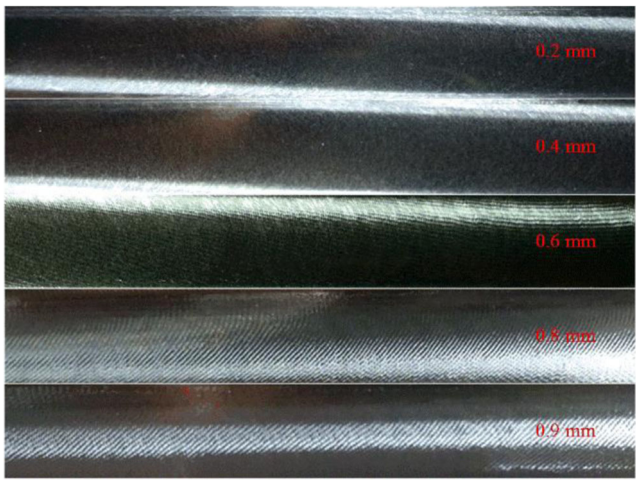

Fig. 9 The finished workpiece surfaces under different cutting conditions (axial cutting depths) in the cutting group II

The 13 frequency domain statistic indicators calculation results and the final finished workpiece surface of different cutting conditions in the cutting group II are shown in Figs. 8 and 9, respectively. Results shown in Figs. 8 and 9 are similar to that of the cutting group I. When the axial cutting depths are 0.2 and 0.4 mm, the milling operation is stable and the finished workpiece surface is very smooth. Slight chatter occurs when the axial cutting depth is 0.6 mm, and there leaves slight chatter marks on the finished surface. When the axial cutting depths increase to 0.8 and 0.9 mm, the chatter vibration aggravate and the finished workpiece surface is very bad. The frequency domain statistic indicators calculation results for both stable and unstable chatter cutting conditions are similar to that of group I. The indicators P1, P2, P6, P10, P12, P13, P3, and P4 can provide a clear identification between stable milling and unstable milling with chatter vibration. However, indicators such as P5, P7, P8, P9, and P11 are not

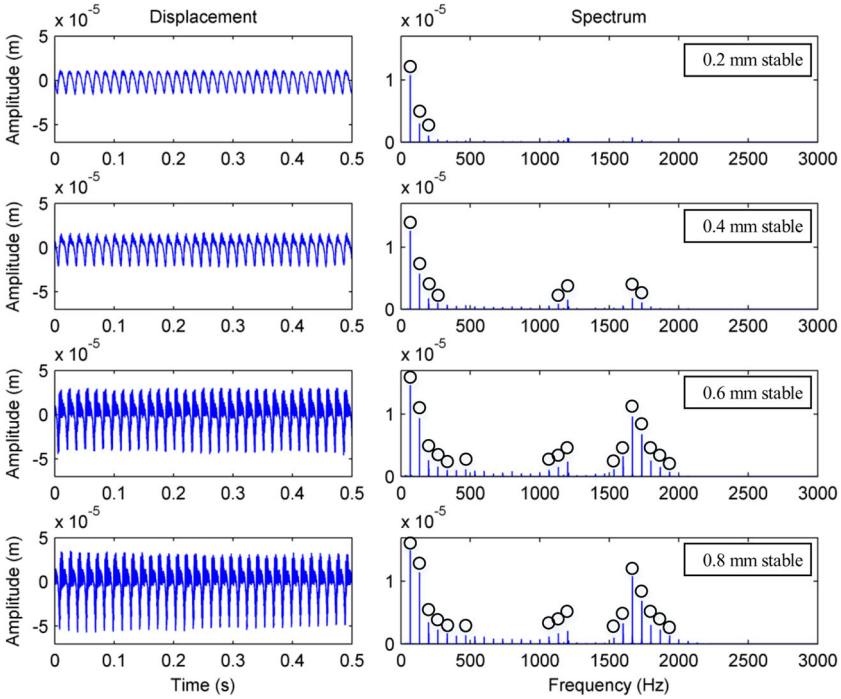

Fig. 10 The time domain waveform and spectrum of the displacement under different cutting conditions in the cutting group III (*white circle* the harmonics of the tooth passing frequency)

suited for chatter identification in the milling process, as shown in Figs. 7 and 8.

The special cutting condition mentioned above in section 2.2.1 appears in the cutting group IIII. The time domain waveform and spectrum of the displacement signal under different cutting conditions in the cutting group III are shown in Fig. 10. The finished workpiece surfaces under different axial cutting depths are shown in Fig. 11. From Fig. 11, it can be seen that the spectrum of displacement signal under all different axial cutting depths are composed of the harmonics of the TPF. When the axial cutting depth is small, the spectrum is mainly composed of low orders of TPF harmonics at the low-frequency region. With the increase of axial cutting depth, the amplitude of the displacement signal increases and more high-order harmonics of the TPF appear at the high-frequency region of the spectrum with their amplitude increasing gradually. The cutting conditions are stable without chatter vibration, and the finished workpiece surfaces are very good as shown in Fig. 11.

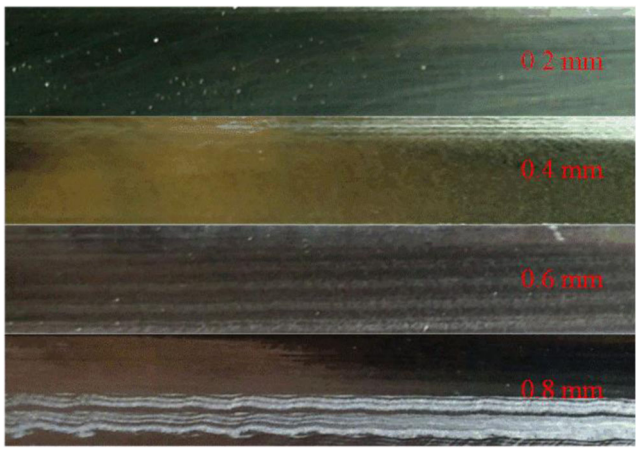

Fig. 11 The finished workpiece surfaces under different cutting conditions in the cutting group III

The 13 frequency domain statistic indicators of the filtered ZST-TFD calculation results are shown in Fig. 12. Indicators P1, P2, P3, P4 P6, P10, P12, and P13 provide excellent results. All the value of these indicators agrees well with the stable cutting condition results of group I and group II, and the effect of the TPF harmonics components has been effectively removed. These indicators can provide effective chatter identification with the consideration of the special cutting conditions mentioned above.

As for the peripheral milling tests in group IV, the 13 frequency domain statistic indicators calculation results of different cutting conditions are shown in Fig. 13, and the finished workpiece surfaces are shown in Fig. 14.

From Fig. 14, it can be seen that when the radial cutting depths are 0.2, 0.5, and 1.0 mm, the peripheral milling processes are stable and the finished workpiece surfaces are very smooth. When the radial cutting depths increase to 2.0, 2.5, and 3.0 mm, the cutting processes become unstable with

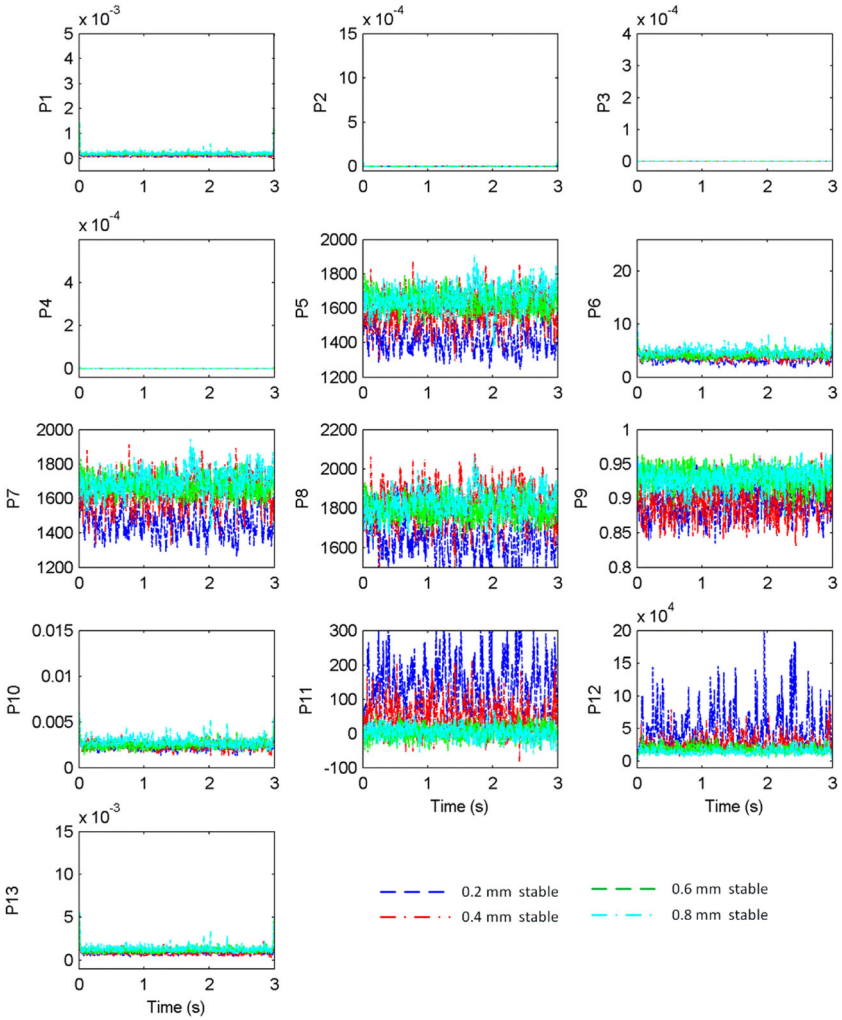

Fig. 12 The 13 frequency domain statistic indicators calculation results of different cutting conditions in the cutting group III

chatter vibration, and the finished workpiece surfaces are very bad with obvious chatter marks.

From Fig. 13, it can be seen that indicators P1, P2, P3, P4, P6, P10, P12, and P13 also provide excellent results. The calculation results of these indicators for both stable and unstable cutting processes agree well with those of the first cutting test groups, i.e., groups I, II, and III.

Synthesizing the results of the above four groups of cutting tests, it can be found that the proposed instantaneous frequency domain statistic indicators based on the filtered ZST-TFD, such as P1, P2, P3, P4, P6, P10, P12, and P13, can provide excellent chatter identification results under different cutting methods (such as end milling and peripheral milling) with different cutting parameters.

The calculation results of the proposed energy ratio indicator ENGR of four different cutting test groups with different cutting parameters are shown in Fig. 15. From Fig. 15, it can be seen that when the cutting condition is stable without chatter vibration, the ENGR indicator is always less than 0.2. However, when the cutting process is unstable with chatter vibration, the value of the ENGR indicators is always larger than 0.4. Additionally, from Fig. 15, it can be found that under the same cutting conditions (stable or unstable), the values of the ENGR indicators always concentrate in a very narrow band, and the indicator values with different cutting parameters always cross with each other. Take group I as example; when the cutting conditions are stable with axial cutting depth as 0.2 and 0.4 mm, the instantaneous ENGR indicators concentrate at the range from 0 to 0.1 and cross with each other. When the cutting conditions are unstable with chatter vibration under axial cutting depths from 0.6 to 1.2 mm, the values of instantaneous ENGR indicators concentrate in the range from 0.55 to 0.65 and cross with each other. For one considered cutting group, the instantaneous energy of both the tooth passing components and the chatter frequency components increases with the increase of the cutting depth, and this is the reason why the difference between the indicator values of different cuttings with chatter vibration is very small. From Fig. 15c,

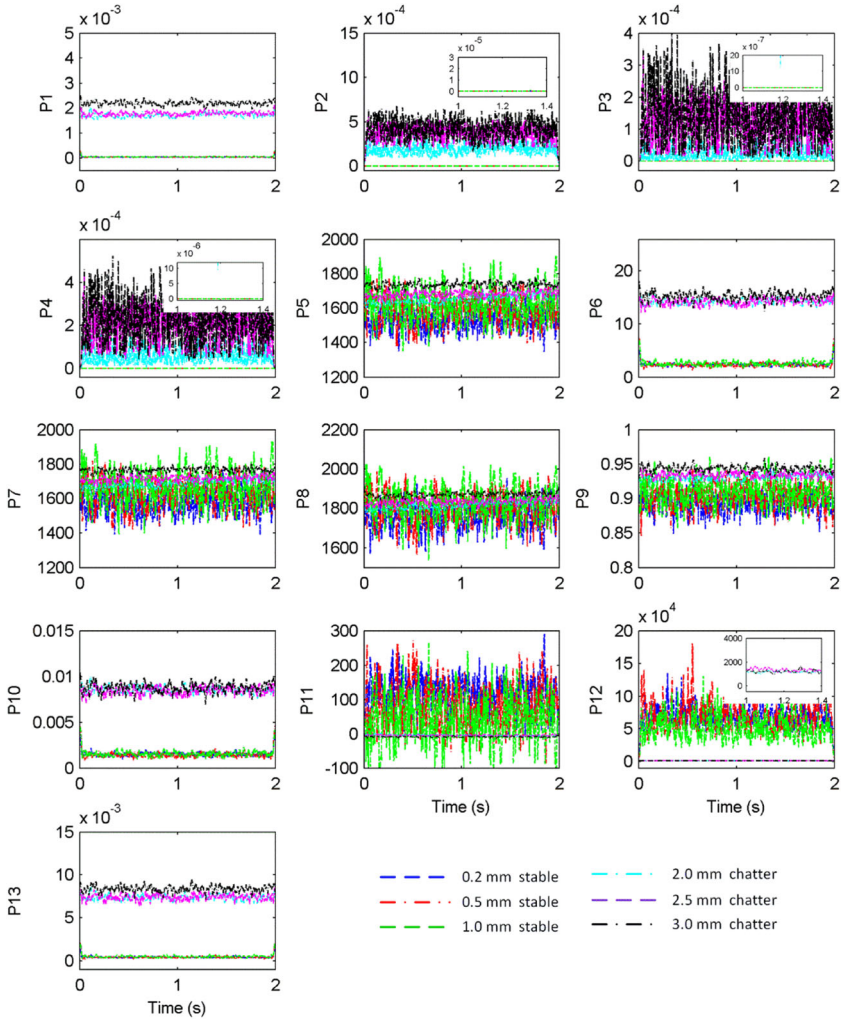

Fig. 13 The 13 frequency domain statistic indicators calculation results of different cutting conditions in the cutting group IV

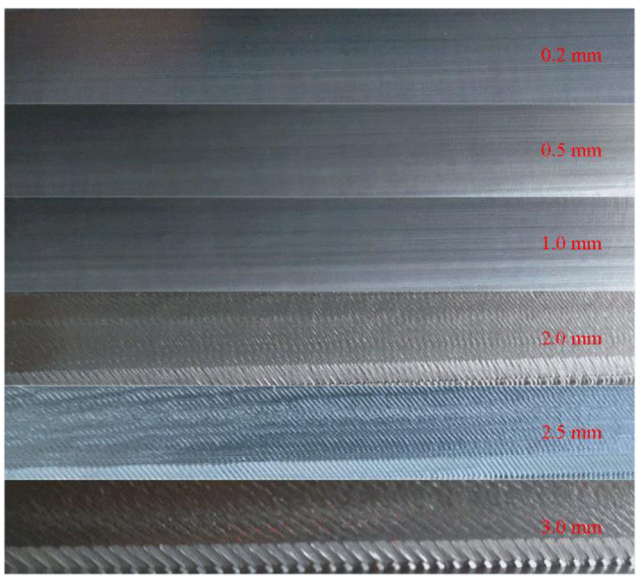

Fig. 14 The finished workpiece surfaces under different cutting conditions in the cutting group IV

it can be seen that the stable condition of the special cutting case can be effectively identified by the proposed instantaneous ENGR indicator.

Above all, from Fig. 15, it can be concluded that the proposed instantaneous ENGR indicator is an effective chatter identification indicator. The special cutting condition can be effectively monitored by the proposed ENGR indicator.

4 Conclusions

This paper presents a milling chatter identification approach combined with the time-frequency analysis method and instantaneous frequency and energy aggregation characteristics of the chatter vibration signal in the milling process.

In this paper, a zoom synchrosqueezing transform time-frequency analysis method is used to process and deal with the time-varying and non-stationary characteristics of the chatter vibration signal in the milling process. The ZST is used as the preprocessing approach to firstly accurately characterize the time-varying and non-stationary characteristics of the

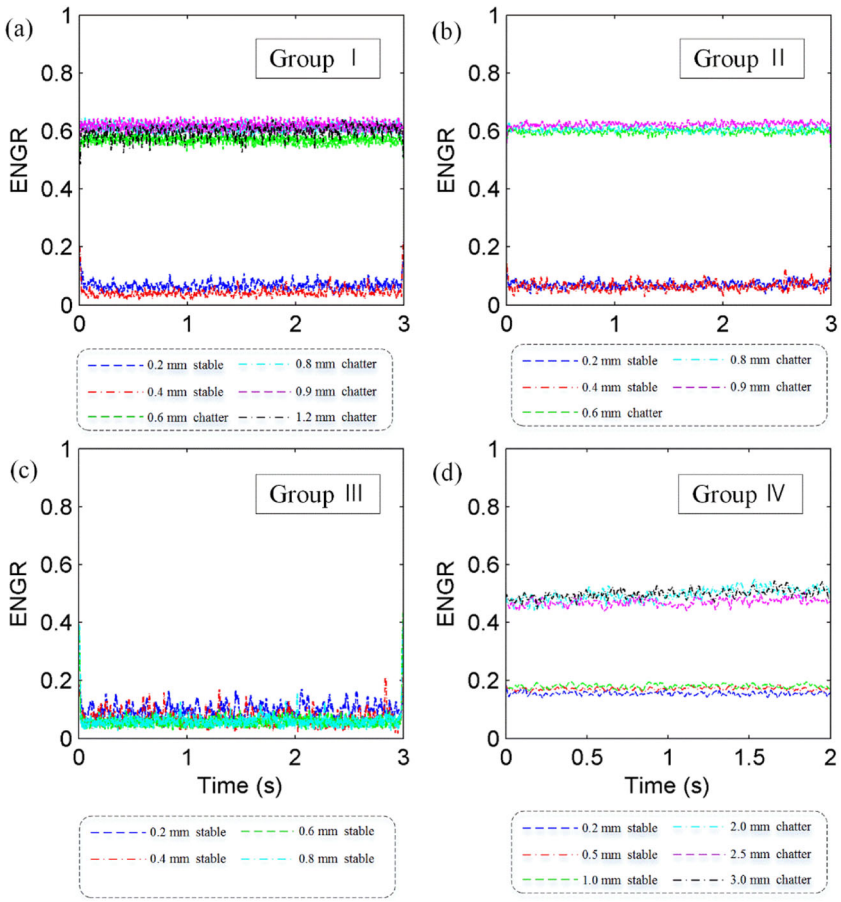

Fig. 15 The ENGR indicators calculation results under different cutting conditions of different cutting groups

milling chatter signal with both excellent time and frequency resolution and to obtain energy concentrated time-frequency distribution. In order to get rid of the influence of the cutting parameters on the effectiveness of the developed chatter detection indicators, the harmonics of the spindle rotating frequency have been filtered from the ZST-TFD.

This paper considers the chatter from the energy aggregation characteristic perspective. Thirteen instantaneous frequency domain statistic indicators and an energy ratio indicator based on the time-frequency distribution obtained by ZST are developed for milling chatter identification. The instantaneous frequency domain statistic and energy ratio of the TFD at a considered transient is used to characterize and monitor the instantaneous frequency and energy distribution of the vibration signal, respectively. Four groups of cutting tests with both end milling and peripheral milling are conducted to validate the effectiveness of the developed chatter identification indicators. The results under different cutting conditions with different cutters indicate that the proposed method can effectively identify the chatter onset in the milling process. The results also indicate that the proposed approach and indicators are insensitive to the cutting parameters. The instantaneous frequency statistic indicators P1, P2, P6, P10, P12, and P13, and the energy ratio indicator ENGR can provide a clear identification between stable milling and unstable milling with chatter vibration, while indicators such as P5, P7, P8, P9, and P11 are not suitable for chatter identification in the milling process.

Acknowledgements The authors would like to acknowledge the support of the National Natural Science Foundation of China (Grant No. 51575423 and 51421004) and Natural Science Foundation of Shaanxi (No. 2017JM5120).

References

1. Quintana G, Ciurana J (2011) Chatter in machining processes: a review. Int J Mach Tools Manuf 51(5):363–376
2. Cao H, Zhang X, Chen X (2017) The concept and progress of intelligent spindles: a review. Int J Mach Tools Manuf 112:21–52
3. Budak E, Altintas Y (1998) Analytical prediction of chatter stability in milling—part I: general formulation. J Dyn Syst Meas Control 120(1):22–30
4. Budak E, Altintas Y (1998) Analytical prediction of chatter stability in milling—part II: application of the general formulation to common milling systems. J Dyn Syst Meas Control 120(1):31–36

5. Altintas Y, Weck M (2004) Chatter stability of metal cutting and grinding. CIRP Ann Manuf Technol 53(2):619–642
6. Insperger T, Stépán G (2002) Semi-discretization method for delayed systems. Int J Numer Methods Eng 55(5):503–518
7. Insperger T, Stépán G (2004) Updated semi-discretization method for periodic delay-differential equations with discrete delay. Int J Numer Methods Eng 61(1):117–141
8. Insperger T, Stépán G, Turi J (2008) On the higher-order semi-discretizations for periodic delayed systems. J Sound Vib 313(1–2):334–341
9. Ding Y, Zhu L, Zhang X, Ding H (2010) A full-discretization method for prediction of milling stability. Int J Mach Tools Manuf 50(5):502–509
10. Wang L, Liang M (2009) Chatter detection based on probability distribution of wavelet modulus maxima. Robot Comput Integr Manuf 25(6):989–998
11. Cao H, Yue Y, Chen X, Zhang X (2017) Chatter detection based on synchrosqueezing transform and statistical indicators in milling process. Int J Adv Manuf Technol:1–12
12. Zhang Z, Li H, Meng G, Tu X, Cheng C (2016) Chatter detection in milling process based on the energy entropy of VMD and WPD. Int J Mach Tools Manuf 108:106–112
13. Cao H, Zhou K, Chen X, Zhang X (2017) Early chatter detection in end milling based on multi-feature fusion and 3σ criterion. Int J Adv Manuf Technol 92(9–12):4387–4397
14. van Dijk NJ, van de Wouw N, Doppenberg EJ, Oosterling HA, Nijmeijer H (2012) Robust active chatter control in the high-speed milling process. IEEE Trans Control Syst Technol 20(4):901–917
15. Wang C, Zhang X, Liu Y, Cao H, Chen X (2018) Stiffness variation method for milling chatter suppression via piezoelectric stack actuators. Int J Mach Tools Manuf 124:53–66
16. Kuljanic E, Sortino M, Totis G (2008) Multisensor approaches for chatter detection in milling. J Sound Vib 312(4):672–693
17. Marinescu I, Axinte DA (2011) An automated monitoring solution for avoiding an increased number of surface anomalies during milling of aerospace alloys. Int J Mach Tools Manuf 51(4):349–357
18. Lamraoui M, Thomas M, El Badaoui M, Girardin F (2014) Indicators for monitoring chatter in milling based on instantaneous angular speeds. Mech Syst Signal Process 44(1):72–85
19. Gradišek J, Govekar E, Grabec I (1998) Using coarse-grained entropy rate to detect chatter in cutting. J Sound Vib 214(5):941–952
20. Yoon M, Chin D (2005) Cutting force monitoring in the endmilling operation for chatter detection. Proc Inst Mech Eng B J Eng Manuf 219(6):455–465
21. Cao H, Lei Y, He Z (2013) Chatter identification in end milling process using wavelet packets and Hilbert–Huang transform. Int J Mach Tools Manuf 69:11–19
22. Cao H, Zhou K, Chen X (2015) Chatter identification in end milling process based on EEMD and nonlinear dimensionless indicators. Int J Mach Tools Manuf 92:52–59
23. Choi T, Shin YC (2003) On-line chatter detection using wavelet-based parameter estimation. J Manuf Sci Eng, Trans ASME 125(1):21–28
24. Fu Y, Zhang Y, Zhou H, Li D, Liu H, Qiao H, Wang X (2016) Timely online chatter detection in end milling process. Mech Syst Signal Process 75:668–688
25. Pérez-Canales D, Álvarez-Ramírez J, Jáuregui-Correa JC, Vela-Martínez L, Herrera-Ruiz G (2011) Identification of dynamic instabilities in machining process using the approximate entropy method. Int J Mach Tools Manuf 51(6):556–564
26. Marinescu I, Axinte DA (2008) A critical analysis of effectiveness of acoustic emission signals to detect tool and workpiece malfunctions in milling operations. Int J Mach Tools Manuf 48(10):1148–1160
27. Kakinuma Y, Sudo Y, Aoyama T (2011) Detection of chatter vibration in end milling applying disturbance observer. CIRP Ann Manuf Technol 60(1):109–112
28. Yamato S, Hirano T, Yamada Y, Koike R, Kakinuma Y (2017) Sensor-less on-line chatter detection in turning process based on phase monitoring using power factor theory. Precis Eng
29. Cao H, Yue Y, Chen X, Zhang X (2017) Chatter detection in milling process based on synchrosqueezing transform of sound signals. Int J Adv Manuf Technol 89(9–12):2747–2755
30. Schmitz TL (2003) Chatter recognition by a statistical evaluation of the synchronously sampled audio signal. J Sound Vib 262(3):721–730
31. Singh KK, Singh R, Kartik V (2015) Comparative study of chatter detection methods for high-speed micromilling of Ti6Al4V. Procedia Manufacturing 1:593–606
32. Rafal R, Pawel L, Krzysztof K, Bogdan K, Jerzy W (2015) Chatter identification methods on the basis of time series measured during titanium superalloy milling. Int J Mech Sci 99:196–207
33. Lamraoui M, Thomas M, El Badaoui M (2014) Cyclostationarity approach for monitoring chatter and tool wear in high speed milling. Mech Syst Signal Process 44(1):177–198
34. Uekita M, Takaya Y (2017) Tool condition monitoring technique for deep-hole drilling of large components based on chatter identification in time–frequency domain. Measurement 103:199–207
35. Li X, Wong Y, Nee A (1997) Tool wear and chatter detection using the coherence function of two crossed accelerations. Int J Mach Tools Manuf 37(4):425–435
36. Suh C, Khurjekar P, Yang B (2002) Characterisation and identification of dynamic instability in milling operation. Mech Syst Signal Process 16(5):853–872
37. Pérez-Canales D, Vela-Martínez L, Jáuregui-Correa JC, Alvarez-Ramirez J (2012) Analysis of the entropy randomness index for machining chatter detection. Int J Mach Tools Manuf 62:39–45
38. Daubechies I, Lu J, Wu H-T (2011) Synchrosqueezed wavelet transforms: an empirical mode decomposition-like tool. Appl Comput Harmon Anal 30(2):243–261
39. Li C, Liang M (2012) A generalized synchrosqueezing transform for enhancing signal time–frequency representation. Signal Process 92(9):2264–2274
40. Oberlin T, Meignen S, Perrier V (2015) Second-order synchrosqueezing transform or invertible reassignment? Towards ideal time-frequency representations. IEEE Trans Signal Process 63(5):1335–1344
41. Xi S, Cao H, Chen X, Zhang X, Jin X (2015) A frequency-shift synchrosqueezing method for instantaneous speed estimation of rotating machinery. J Manuf Sci Eng 137(3):031012
42. Cao H, Xi S, Chen X, Wang S (2016) Zoom synchrosqueezing transform and iterative demodulation: methods with application. Mech Syst Signal Process 72:695–711
43. Xi S, Cao H, Chen X (2016) Zoom synchrosqueezing transform for instantaneous speed estimation of high speed spindle. Mater Sci Forum
44. Wang S, Chen X, Cai G, Chen B, Li X, He Z (2014) Matching demodulation transform and synchrosqueezing in time-frequency analysis. IEEE Trans Signal Process 62(1):69–84
45. Obuchowski J, Wyłomańska A, Zimroz R (2014) The local maxima method for enhancement of time–frequency map and its application to local damage detection in rotating machines. Mech Syst Signal Process 46(2):389–405
46. Yao Z, Mei D, Chen Z (2010) On-line chatter detection and identification based on wavelet and support vector machine. J Mater Process Technol 210(5):713–719
47. Liu C, Zhu L, Ni C (2017) The chatter identification in end milling based on combining EMD and WPD. Int J Adv Manuf Technol 91(9–12): 3339–3348
48. Liu C, Zhu L, Ni C (2018) Chatter detection in milling process based on VMD and energy entropy[J]. Mech Syst Signal Process 105: 169–182